Asian Journal of Physics
Vol. 31, Nos 3-6 (2022) 401-417
Available on: www.asianjournalofphysics.com

ap

Optical wave propagation in graded-index waveguides

Govind P Agrawal*

The Institute of Optics, University of Rochester, Rochester ,NY,14627,USA

Refractive index inside a graded-index (GRIN) waveguide is not uniform but decreases in the radial direction in a nearly parabolic fashion. It is this index gradient that confines light to the waveguide's core. Wave propagation in GRIN fibers was studied during the 1970s, motivated by their applications in optical communication systems. More recently, GRIN fibers have been used to study the spatiotemporal nonlinear phenomena. This article focuses on the propagation of pulsed optical beams in GRIN waveguides. The modes of a GRIN medium with a parabolic index profile are used to the self-imaging phenomenon that is unique to GRIN waveguides. Evolution of a pulsed Gaussian beam is considered using a non-modal approach, resulting in a four-dimensional propagation equation. It is extended to include the Kerr nonlinearity, responsible for both the self-focusing and self-phase modulation. The resulting equation is solved approximately to obtain an effective nonlinear Schrodinger equation that includes the effects of self-imaging. This equation is used to discuss the formation of fundamental and higher order solitons inside GRIN waveguides. The impact of intrapulse Raman scattering is also considered.

Keywords: Optical waveguides, Graded-index fibers, Optical Solitons, Raman scattering.

1 Introduction

I met Bishnu Pal first time in 1971, when I joined the Ph D program of the Indian Institute of Technology (IIT) in New Delhi, India. We both left IIT Delhi for Europe after completing our Ph D degrees in optics and photonics, but our friendship has continued to this day. It is with great pleasure that I contribute this article to the special issue of the Asian Journal of Physics being published to honor Prof Bishnu Pal.

I have chosen graded-index waveguides as the topic of this article because it was Bishnu who introduced me to graded-index (GRIN) fibers. Such fibers were developed around the year 1970 and were a hot topic of study during my Ph D years at IIT Delhi. Prof Ajoy Ghatak was Bishnu's thesis adviser. He was also my teacher during my M Sc studies and acted as my mentor during the Ph D years. Even though Prof Ghatak was not my thesis adviser, I coauthored a paper with him that was published in November 1974 [1]. This paper is being cited even after 48 years because it remains relevant to the current research on GRIN fibers. I am indebted to Prof Ghatak and Prof Pal for introducing me to the field of optical waveguides in general, and to GRIN fibers in particular.

GRIN fibers contain a central core, where the refractive index is not uniform and decreases parabolically in the radial direction. In contrast to the step-index fibers, it is the index gradient that confines light to the waveguide. Wave propagation in GRIN fibers was studied during the 1970s, motivated mostly by their applications in optical Communication systems [2-5]. Even though GRIN fibers were initially used for such systems, the use of single-mode fibers became dominant after 1985. It was only after 2010 that multimode fibers attracted renewed attention for enhancing the capacity of optical communication systems through space-division multiplexing [6-8]. This revival led to a resurgence of interest in GRIN fibers,

Corresponding author
e mail: govind.agrawal@rochester.edu (Govind P Agrawal)

especially in their nonlinear properties [9-14]. Among the nonlinear phenomena that have attracted attention is the issue of formation of solitons inside multimode fibers.

The soliton issue was addressed as early as 1980 in several publications [15,16]. Theoretical work carried out during the 1990s indicated that the formation of temporal solitons was indeed feasible inside a GRIN medium [17-19]. It eventually led in 2013 to the observation of such a soliton [10]. In this experiment, only three lowest-order modes of the fiber were excited. It was shown in 2018 that GRIN fibers support propagation of temporal solitons even when a large number of modes participate in their formation [20], but their spatial width oscillates along the fiber because of periodic self-imaging [21]. Since then, much work has been done to understand the formation of solitons inside GRIN fibers [22-24].

The article is organized as follows. In Section 2, the modes of a GRIN waveguide with a parabolic index profile are discussed, and the ladder-like structure of their propagation constants is emphasized. Section 3 is devoted to the self-imaging phenomenon that is unique to GRIN waveguides. A modal-expansion aproach is used to show that the optical field at any point inside the waveguide can be obtained, without any reference to the underlying modes [1]. This result is used in Section 4 to study the propagation of Gaussian beams inside a GRIN waveguide, and it is shown that the beam's width varies in a periodic fashion. The case of an off-center Gaussian beam is also discussed. Evolution of a pulsed Gaussian beam is considered in Section 5 using a non-modal approach, resulting in a four-dimensional propagation equation. This equation is extended in Section 6 to include the Kerr-type nonlinearity, responsible for both the self-focusing and self-phase modulation (SPM). It is solved approximately to obtain an effective nonlinear Schrödinger (NLS)equation that includes the effects of periodic self-imaging. Section 7 is devoted to the topic of spatiotemporal solitons forming inside GRIN waveguides. The main results are summarized in Section 8.

2 Wave propagation in GRIN media

It is often simpler to solve Maxwell's equations in the frequency domain. For this purpose, we define the Fourier transform of the electric field $\mathbf{E}(\mathbf{r}, t)$ as

$$\tilde{\mathbf{E}}(\mathbf{r},\omega) = \int_{-\infty}^{\infty} \mathbf{E}(\mathbf{r},t)\, e^{i\omega t} dt. \tag{1}$$

Maxwell'sequations in the frequency domain are then combined to obtain the following equation:

$$\nabla \times \nabla \times \tilde{\mathbf{E}} = \mu_0 \varepsilon\, \omega^2\, \tilde{\mathbf{E}}. \tag{2}$$

Keeping in mind that ε is not a constant for a GRIN medium, we can write this equation in the form

$$\nabla^2 \tilde{\mathbf{E}} + \mu_0 \varepsilon\, \omega^2\, \tilde{\mathbf{E}} + \nabla \left(\frac{1}{\varepsilon} \nabla \varepsilon \cdot \tilde{\mathbf{E}} \right) = 0.\ \mathbf{E} \tag{3}$$

Using $\varepsilon = \varepsilon_0 n^2(\mathbf{r})$, where n is the refractive index, together with $\mu_0 \varepsilon_0 = 1/c^2$, Eq (3) becomes

$$\nabla^2 \tilde{\mathbf{E}} + n^2(\mathbf{r})\, k_0^2\, \tilde{\mathbf{E}} + \nabla \left(\frac{1}{n^2} \nabla n^2 \cdot \tilde{\mathbf{E}} \right) = 0, \tag{4}$$

where, $k_0 = \omega/c = 2\pi/\lambda$ is related to the wave length of radiation.

The last term in Eq (4) is finite because the index gradient ∇n is not zero for a GRIN medium. It has been found in recent years that this term leads to the optical analog of the spin-orbit coupling for vortex beams carrying the orbital angular momentum [25,26]. Its magnitude is, however, negligible when the refractive index $n(\mathbf{r})$ varies on a spatial scale much longer than a wavelength.We assume this to be the case and focus on the simpler Helmholtz equation

$$\nabla^2 \tilde{\mathbf{E}} + n^2(\mathbf{r})\, k_0^2\, \tilde{\mathbf{E}} = 0. \tag{5}$$

The refractive index of GRIN fibers decreases radially inside the core of radius a from its value n_0 at the center to the cladding value n_c as

$$n^2(\mathbf{r}) = n_0^2 [1 - 2\Delta\, (x^2 + y^2)/a^2], \tag{6}$$

where, $\Delta = (n_1 - n_c)/n_1$ plays an important role and is defined in the same way as for step-index fibers [8]. To obtain ananalytic solution, it is necessary to assume that Eq (6) applies for all values $\rho = (x^2 + y^2)^{1/2}$. Figure 1 shows the nature of this approximation by comparing the actual profile of a GRIN medium to a parabolic shape.

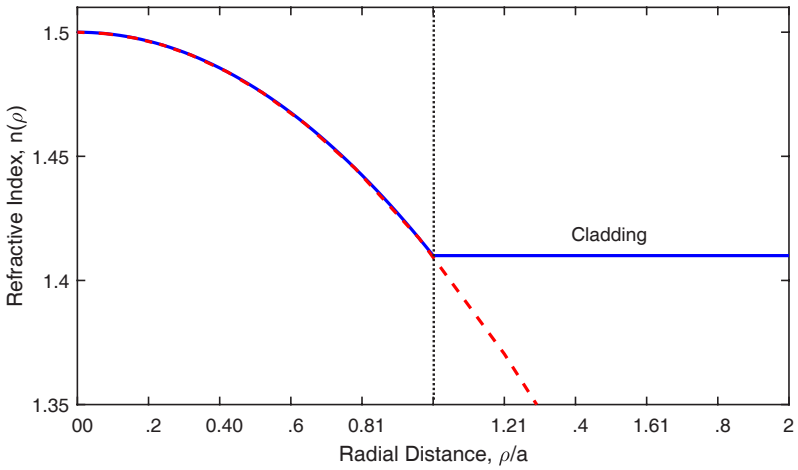

Fig 1. Actual index profile of a GRIN fiber (solid line) is compared to its parabolic approximation (dashed line).The dotted vertical line marks the core-cladding boundary.

There are two ways of solving Eq (5). We can solve it as an initial-value problem, where $\tilde{\mathbf{E}}$ is specified at the input end of a GRIN medium located at $z = 0$. Alternatively, we can adopt the modal approach in which Eq (5) is solved as an eigenvalue problem, whose eigenfunctions, called optical modes, do not change with z. We follow the modal approach and assume that any solution of Eq (5) has the form

$$\tilde{\mathbf{E}} = \hat{\mathbf{p}}\, U(x,y)\, e^{i\beta z}, \quad (7)$$

where $\hat{\mathbf{p}}$ is the polarization unit vector, $U(x, y)$ is the eigenfunction, and β is the propagation constant (or eigenvalue) that is yet to be determined. Using $n(\mathbf{r})$ from Eq (6), Eq (5) for a GRIN medium is reduced to

$$\frac{d^2U}{dx^2} + \frac{d^2U}{dy^2} + \{n_0^2 k_0^2 [1 - 2\Delta(x^2 + y^2)/a^2] - \beta^2\} U = 0. \quad (8)$$

The preceding equation can be solved with the method of separation of variables. Its general solution takes the form [27]

$$U_{mn}(x,y) = \left[N_m H_m(qx) \exp\left(-\frac{1}{2} q^2 x^2\right)\right]\left[N_n H_n(qy) \exp\left(-\frac{1}{2} q^2 y^2\right)\right], \quad (9)$$

where the integers, m and n, start at 0, $q^2 = n_0 k_0 \sqrt{2\Delta}/a$, $H_m(qx)$ is a Hermite polynomial of the m^{th} order, and N_m is a normalization constant such that

$$\int\int_{-\infty}^{\infty} U^*_{m'n'}(x,y)\, U_{mn}(x,y)\, dx\, dy = \delta_{m'm}\, \delta_{n'n}. \quad (10)$$

Each Hermite-Gauss mode is denoted by HG_{mn} and its propagation constant depends on the GRIN parameters as

$$\beta_{mn} = n_0 k_0 [1 - (m + n + 1)(4\Delta/V)]^{1/2}, \quad (11)$$

where, similar to the case of step-index fibers, we defined a dimensionless parameter V, as

$$V = (qa)^2 = n_0 k_0 a \sqrt{2\Delta}. \quad (12)$$

The value of this parameter exceeds 20 for GRIN fibers designed with a = 25μm, and the total number of modes scales as $V^2/4$ for such fibers. As the ratio Δ/V is relatively small ($< 10^{-3}$), the second term

in Eq (11) remains small compared to 1, if we limit $m+n$ to values well below1000. By making a binomial expansion, we can approximate β_{mn} as

$$\beta_{mn} \approx k_0 [n_0 - (m + n + 1)\, \delta n], \qquad \delta n = 2n_0 \Delta / V. \tag{13}$$

It is common to define an effective mode index as, $\bar{n} = \beta / k_0$. If we introduce a single integer as $g = m + n + 1$, we can write it in the simple form, $\bar{n}_g = n_0 - g\delta n$, where g labels different mode groups.

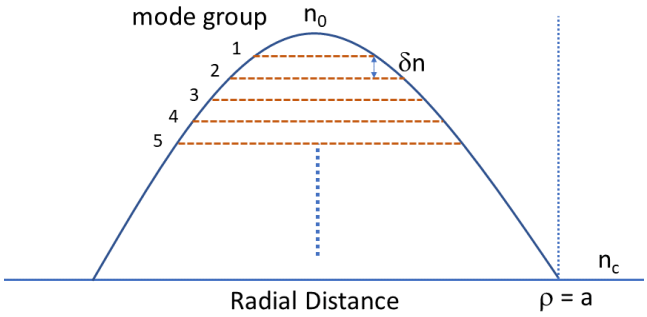

Fig 2. Schematic showing the effective mode indices (dashed lines) for several mode groups within parabolic profile of a GRIN medium. The dotted vertical line at ρ = a marks its core-cladding boundary.

Figure 2 shows schematically the ladder-like structure of $\bar{n}_g$ values for several mode groups within the parabolic profile of a GRIN medium. The first group for $g = 1$ contains the HG_{00} mode with the largest value $\bar{n}_1 = n_0 \delta n$; this mode is called the fundamental mode. As m and n change such that g increases by 1, $\bar{n}_g$ decreases by the same amount δn. The largest value of the integer g is set by the condition that $\bar{n}_g$ must remain larger than the cladding index $n_c = n_0(1 - \Delta)$ for the modes to remain confined within the core of the GRIN medium. The ladder-like structure of the eigen values is analogous to the energy levels of a harmonic oscillator and is a consequence of the parabolic nature of the index profile. It leads to a phenomenon called self-imaging, which manifests as periodic focusing and defocusing of an optical beam inside a GRIN medium such that the input shape of the beam is reproduced at certain locations [21].

3 Propagation Kernel of GRIN media

Let us first consider the propagation of a continuous-wave (CW) beam entering a GRIN medium at $z = 0$ with an electric field $E(x, y, 0)$. It excites multiple modes such that

$$E(x, y, 0) = \sum_m \sum_n c_{mn} U_{mn}(x, y), \tag{14}$$

where the double sum extends over all modes.The expansion coefficients c_{mn} are found by multiplying this equation with $U^*_{m'n'}(x,y)$ and integrating over the entire transverse plane. Using the orthogonality of modes indicated in Eq (10), we obtain

$$c_{mn} = \iint_{-\infty}^{\infty} U^*_{mn}(x,y)\, E(x, y, 0)\, dx\, dy. \tag{15}$$

As all modes propagate without change in their spatial profiles and only acquire a z-dependent phase shift with propagation inside the GRIN medium, $E(x, y, z)$ is obtained by multiplying each mode with a phase factor such that

$$E(x, y, 0) = \sum_m \sum_n c_{mn} U_{mn}(x,y) \exp(i\beta_{mn} z). \tag{16}$$

Substituting c_{mn} from Eq (15), we can write the result in the form

$$E(x, y, z) = \iint_{-\infty}^{\infty} K(x, x'; y, y')\, E(x', y', 0)\, dx'\, dy', \tag{17}$$

where the propagation kernel is given by

$$K(x, x'; y, y') = \sum_m \sum_n U_{mn}(x,y)\, U^*_{mn}(x',y')\, e^{i\beta_{mn}z}. \tag{18}$$

It was found in 1974 that the double sum in Eq (18) can be carried out for GRIN fibers because of the ladder-like structure of the modal propagation constants [1].The final result is given by

$$K(x, x'; y, y') = \frac{k}{2\pi i}\left(\frac{be^{i\psi}}{\sin(bz)}\right) \exp\left(\frac{ikb}{2\sin(bz)}[\cos(bz)(x'^2 + y'^2) - 2(xx' + yy')]\right), \tag{19}$$

where $k = n_1 k_0$, $b = \sqrt{2\Delta}/a$, and the phase ψ varies as

$$\psi(x, y, z) = kz + \frac{1}{2}\, k\, b \cot(bz)\, (x^2 + y^2). \tag{20}$$

Noting that $\sin(bz)/b = z$ in the limit $b \to 0$, it is easy to see that the kernel in Eq (19) reduces to

$$K_h(x, x'; y, y') = \frac{k e^{ikz}}{2\pi i z} \exp\left(\frac{ik}{2z}\,[(x - x')^2 + (y - y')^2]\right), \tag{21}$$

which is the form expected for a homogeneous medium of constant refractive index.

It is well known that a GRIN fiber reproduces its input field periodically along its length.This self-imaging property follows from the observation that the Kernel in Eq (19) is reduced to the form

$$K(x, x'; y, y') = \delta(x - x')\, \delta(y - y')\, e^{ikz} \tag{22}$$

at distances that are integer multiples of the fundamental period $2\pi/b$.This can be seen by noting that $\cos(bz) = 1$ at such distances and K in Eq (19) can be written as $K = f(x - x')\, f(y - y')\, e^{ikz}$, where the function $f(x)$ is defined as

$$f(x) = \sqrt{\frac{p}{\pi}}\, e^{-px^2}, \quad p = \frac{kb}{2i\sin(bz)}. \tag{23}$$

It is easy to show that $\int_{-\infty}^{\infty} f(x)\, dx = 1$. At distances $z = 2m\pi/b$, where m is an integer, p becomes infinitely large, and $f(x)$ is reduced to the delta function $\delta(x)$.

It follows from Eqs (17) and (22) that the field $E(\mathbf{r})$ becomes identical to the input field at all such distances, resulting in self-imaging.The self-imaging period,

$$L_p = \frac{2\pi}{b} = \frac{2\pi a}{\sqrt{2\Delta}}, \tag{24}$$

depends only on the two GRIN parameters, a and Δ, and is typically ~1 mm for standard GRIN fibers. Self-imaging also occurs in the middle of each period, with one major difference. In this case, the delta functions in Eq (22) are replaced with $\delta(x + x')$ and $\delta(y + y')$. As a result, $E(x, y, L_p/2) = E(-x, -y, 0)$, i.e.,the image is flipped in both transverse dimensions. If the input field is radially symmetric, the sign change has no impact, and the input field is reproduced (or self-imaged) for the first time at the distance $L_p/2$.

4 Gaussian-beam propagation

As a simple example, we consider the propagation of a Gaussian beam through a GRIN fiber and choose the input field at $z = 0$, to be

$$E(x, y, 0) = A_0 \exp[-(x^2 + y^2)/2w_0^2], \tag{25}$$

where, A_0 is the peak amplitude and w_0 is the initial spot size of the Gaussian beam. We find the electric field at any point inside the GRIN medium by using Eq (25) in Eq (17) together with the propagation kernel in Eq (19). The result can be written as

$$E(\mathbf{r}) = \frac{A_0 k}{2\pi i}\left(\frac{be^{i\psi}}{\sin(bz)}\right) H(x, x')H(y, y'), \tag{26}$$

where the function $H(x, x')$ is defined as

$$H(x, x') = \int_{-\infty}^{\infty} \exp\left(-\frac{x'^2}{2w_0^2} + \frac{ikb}{2\sin(bz)}[\cos(bz)\, x'^2 - 2xx']\right)dx', \tag{27}$$

The preceding integral can be done easily with the final result [21]

$$E(\mathbf{r}) = A_0 F(\mathbf{r}) \exp[i\phi(\mathbf{r})], \tag{28}$$

where the beam's spatial profile retains its Gaussian form,

$$F(\mathbf{r}) = \frac{w_0}{w(z)} \exp\left[-\frac{x^2 + y^2}{2w^2(z)}\right]. \tag{29}$$

and its phase $\phi(\mathbf{r})$ is given by

$$\phi(\mathbf{r}) = \frac{k}{2w}\frac{dw}{dz}(x^2 + y^2) + kz + \tan^{-1}(C_f \tan bz). \tag{30}$$

The spot size $w(z)$ in Eq (29) evolves with z inside the GRIN medium in a periodic fashion as

$$w(z) = w_0 [\cos^2(2\pi z/L_p) + C_f^2 \sin^2(2\pi z/L_p)]^{1/2}, \tag{31}$$

where the parameter C_f is defined as

$$C_f = L_p/(2\pi k w_0^2). \tag{32}$$

These results show that the amplitude, the width, and the phase of a Gaussian beam evolve in a periodic fashion such that the beam recovers all of its input features periodically at distances $z = m(L_p/2)$ (m is any positive integer) because of the self-imaging phenomenon. At distances $z = (m - 1/2)L_p/2$, the beam's width takes its minimum value $w_0 C_f$. The reduction in width is similar to the action of a lens. The focal length, $L_f = L_p/4$, of a GRIN lens is defined as the shortest distance at which the beam first comes to a focus. If we use a = 1mm and $\Delta = 0.05$ as typical values for a GRIN rod, the numerical value of L_f is close to 5mm.

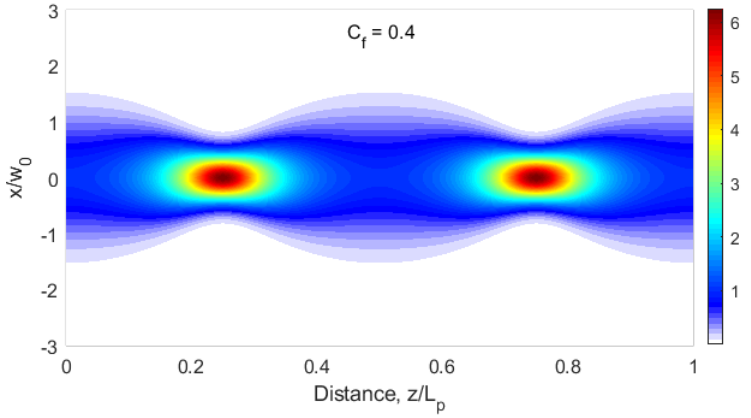

Fig 3. Evolution of an on-axis Gaussian beam inside a GRIN fiber over one self-imaging period. Beam's cross section along the $y = 0$ plane is shown for $C_f = 0.4$.

As an example, Fig 3 shows the evolution of a Gaussian beam over one self-imaging period using $C_f = 0.4$. For this value of C_f, the beam width is reduced by a factor of 2.5 at the point of maximum compression and its peak intensity is enhanced by a factor of 6.25. Compression by a factor of 10 and intensity enhancement by a factor of 100 can be realized by making $C_f = 0.1$.

The Gaussian beam described by Eq (25) is launched such that its center coincides with the core's central axis, and its intensity profile is radially symmetric around this axis. In the modal picture, only radially

symmetric modes are excited by such an input beam. If the peak of the Gaussian beam is shifted by a distance s along the x axis, the input field in Eq (25) is replaced with

$$E(x, y, 0) = A_0 \exp\left(-\left[(x-s)^2 + y^2\right] / 2w_0^2\right). \tag{33}$$

The optical field at any point $\mathbf{r} = (x, y, z)$ is found using Eq (33) in Eq (17) together with the kernel in Eq (19).The final result has the form given in Eq (28), but the beam's amplitude is now governed by [14]

$$F(\mathbf{r}) = \frac{w_0}{w(z)} \exp\left(-\frac{1}{2w^2(z)}\left[(x - s\cos bz)^2 + (y - s\sin bz)^2\right]\right), \tag{34}$$

where, $w(z)$ varies with z in a periodic fashion as indicated in Eq (31).

Figure 4 shows how an off-axis Gaussian beam evolves over one self-imaging period by plotting its intensity variations over one period after choosing $s = w_0$ and $C_f = 0.4$. Similar to the on-axis launch, the beam's width oscillates with z, compressing and recovering its input value periodically. The new feature is that the beam's center also oscillates in a helical fashion around the fiber's axis. Even though the Gaussian beam in Fig 4 recovers its initial width w_0 at $z = L_p/2$, its center is located on the opposite site at $x = s$, resulting in a flipped image. The self-imaging period for a shifted Gaussian beam doubles because its intensity distribution is not radially symmetric around the GRIN rod's axis.

5 Pulse propagation in GRIN fibers

When a pulsed beam is launched into a GRIN fiber, its spatial width continues to evolve periodically and exhibit self-imaging. However, one must consider the dispersion-induced reshaping and broadening of each pulse. A model approach was employed during the 1970s for this purpose, and it was useful to include the effects of random mode coupling along the fiber's length [28-30]. Here, we focus on a non-model

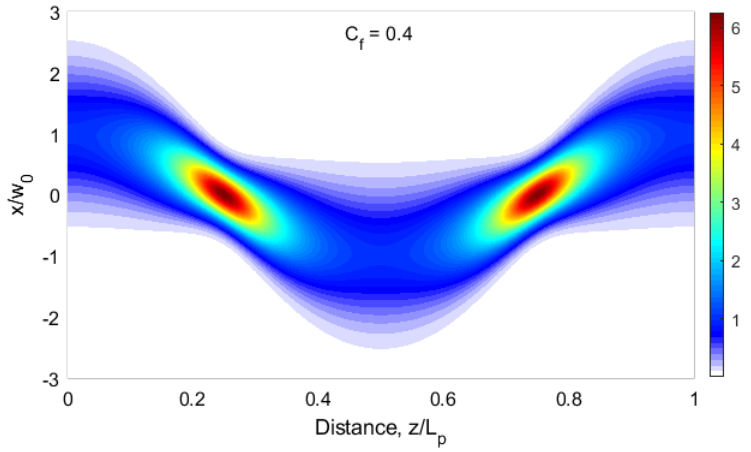

Fig 4. Evolution of an off-axis Gaussian beam (centered at $x = w_0$) inside a GRIN fiber over one self-imaging period. Beam's cross section along the $y = 0$ plane is shown for $C_f = 0.4$.

approach that is useful when mode coupling is negligible. In this case, Eq (5) applies to each spectral component of the pulse and is solved using

$$\tilde{\mathbf{E}}(\mathbf{r},\omega) = \hat{\mathbf{p}}\,\tilde{A}(\mathbf{r},\omega)\exp\left[i\beta(\omega)\,z\right), \tag{35}$$

where, $\beta(\omega) = n_0(\omega)\omega/c$ is the propagation constant. If we neglect the second derivative d^2A/z^2 in the paraxial approximation, $\tilde{A}(\mathbf{r}, \omega)$ satisfies

$$2i\beta(\omega)\frac{\partial \tilde{A}}{\partial z} + \frac{\partial^2 \tilde{A}}{\partial x^2} + \frac{\partial^2 \tilde{A}}{\partial y^2} - 2\Delta\frac{\beta^2}{a^2}(x^2 + y^2)\,\tilde{A}(\mathbf{r},\omega) = 0 \tag{36}$$

Its inverse Fourier transform,

$$A(\mathbf{r}, t) = \frac{1}{2\pi}\int_{-\infty}^{\infty} \tilde{A}(\mathbf{r},\omega)\, \exp[i(\beta - \beta_0)\, z - i(\omega - \omega_0)t]d\omega. \tag{37}$$

then provides us with the spatial as well as temporal dependence of the slowly varying amplitude.

It is useful to convert Eq (36) to the time domain. We use the preceding equation to calculate the spatial derivative,

$$\frac{\partial A}{\partial z} = \frac{1}{2\pi}\int_{-\infty}^{\infty} \left[\frac{\partial \tilde{A}}{\partial z} + i(\beta - \beta_0)\, \tilde{A}\right] \exp[i(\beta - \beta_0)\, z - i\,(\omega - \omega_0)t]\, d\omega. \tag{38}$$

We substitute $\frac{\partial \tilde{A}}{\partial z}$ from Eq (36) and approximate $\beta(\omega)$ with itsTaylor expansion around the central frequency ω_0 in the form $\beta(\omega) = \beta_0 + \beta_1\, \Omega + \frac{1}{2}\, \beta_2\, \Omega^2$, where $\Omega = \omega - \omega_0$. With this simplification, the frequency integration in Eq (38) can be done to obtain thefollowing four-dimensional equation:

$$\frac{\partial A}{\partial z} + \frac{1}{2i\beta_0}\left(\frac{\partial^2 A}{\partial x^2} + \frac{\partial^2 A}{\partial y^2}\right) + \beta_1 \frac{\partial A}{\partial t} + \frac{i\beta_2}{2}\frac{\partial^2 A}{\partial t^2} + \frac{i\beta_0 \Delta}{a^2}(x^2 + y^2)A = 0. \tag{39}$$

Equation (39) governs the spatiotemporal evolution of a pulsed optical beam inside a GRIN medium. Its main advantage is that it includes all modes of a GRIN medium automatically.

We can simplify the four-dimensional problem by considering the length scales associated with the spatial and temporal evolutions. The length scale of spatial changes is provided by the self-imaging period L_p given in Eq (24), with a typical value 1 mm for GRIN fibers. The length scale of temporal evolution is governed by the dispersion length L_D, defined as $L_D = T_0^2/|\beta_2|$, where T_0 is a measure of pulse duration. When, $T_0 = 1$ps, this length is 100m for typical values of β_2 of GRIN fibers at wavelengths near 1550nm.

The vast disparity in the two length scales implies that spatial evolution of a pulsed beam is not much affected by the GVD effects for pulses with a narrow bandwidth such that $\Delta\omega \ll \omega_0$. In contrast, the spatial self-imaging effects may influence the temporal effects. A simple way to implement this idea is to decouple the spatial effects with the approximation

$$\tilde{A}(\mathbf{r}, \omega) \approx F(\mathbf{r}, \omega_0)\, \tilde{A}_t(z, \omega), \tag{40}$$

where the spatial distribution of the beam is at the central frequency ω_0. This is justified for a narrow-bandwidth pulse for which the spatial self-imaging features do not vary much over its bandwidth [31]. Using again the Taylor expansion for $\beta(\omega)$, we find that $A_t(z, t)$ satisfies the one-dimensional equation

$$\frac{\partial A_t}{\partial z} + \beta_1 \frac{\partial A_t}{\partial t} + \frac{i}{2}\beta_2 \frac{\partial^2 A_t}{\partial t^2} = 0. \tag{41}$$

This equation is identical to the one used single-mode fibers and implies that self-imaging does not affect the pulse's evolution. We will see later that this is not the case when nonlinear effects are considered.

One should consider the conditions under which the use of Eq (41) is justified. As a modal approach was not used, it contains only two dispersion parameters, β_1 and β_2, calculated at the central wavelength of the pulsed beam. Also, the spatial and temporal features evolve independently, without any coupling between them. In spite of these simplifications, it represents a valid solution (i) when the input beam excites a large number of modes,(ii) bandwidth of pulses is small relative to the central frequency of the optical spectrum, and (iii) mode coupling is negligible.

6 Nonlinear propagation equation

The refractive index of any material increases slightly at high intensities because of the Kerr effect such that $n(\mathbf{r}, I) = n(\mathbf{r}) + n_2 I$, where I is the local intensity. The parameter n_2 is called the Kerr coefficient, and

its numerical value is about 3×10^{-20}m^2/W for silica glass. The physical origin of the Kerr nonlinearity lies in the anharmonic response of electrons to electromagnetic fields.

Equation (39), governing the spatiotemporal evolution of a pulsed optical beam inside a linear GRIN medium, can be extended to the nonlinear case by adding the following nonlinear term to it:

$$\frac{\partial A}{\partial z}+\frac{1}{2i\beta_0}\left(\frac{\partial^2 A}{\partial x^2}+\frac{\partial^2 A}{\partial y^2}\right)+\beta_1\frac{\partial A}{\partial t}+\frac{i\beta_2}{2}\frac{\partial^2 A}{\partial t^2}+\frac{i\beta_0\Delta}{a^2}(x^2+y^2)A=ik_0n_2|A|^2A. \tag{42}$$

This equation governs the spatiotemporal evolution of optical pulses inside a nonlinear GRIN medium and includes simultaneously the effects of diffraction, dispersion, and the Kerr nonlinearity. The β_1 term does not play an important role because it can be removed by a simple scaling of time, $T = t - \beta_1 z$.

It is not easy to solve Eq (42) analytically, and its numerical solutions are time-consuming because of its multi-dimensional nature. To get some physical insight, consider first the case of a homogeneous medium by setting $\Delta = 0$ in Eq (42). If we neglect the diffraction terms for an optical beam with a large spatial size and use $T = t - \beta_1 z$, we obtain the usual NLS equation:

$$\frac{\partial A}{\partial z}+\frac{i\beta_2}{2}\frac{\partial^2 A}{\partial T^2}=ik_0n_2|A|^2A. \tag{43}$$

This well-known equation has been studied in many different contexts and can be solved exactly with the inverse-scattering method to find specific solutions known as solitons [19]. In the context of optical fibers, solitons represent pulses whose shape either does not change along the fiber, or follows a periodic evolution pattern [14]. Their formation requires negative values of β_2 that correspond to the group-velocity dispersion (GVD) being anomalous.

When diffraction terms are added to Eq (43), we obtain Eq (42) without the GRIN term ($\Delta = 0$). The soliton-like solutions of this equation were investigated during the 1990s and are called spatiotemporal solitons,or optical bullets, because of their confinement in both space and time [19]. Similar to the case of Eq (43), such solitons requires anomalous GVD. However, unlike Eq (43), they are not stable beacuse of the self-focusing effects. One should ask whether Eq (42), describing pulse evolution inside a nonlinear GRIN medium, has stable solutions in the form of a spatiotemporal soliton. Such solutions were investigated during the 1990s by solving Eq (42) with the variational method [17,18]. It was found that their stability is improved by the GRIN nature of the medium, but they are only stable marginally.

The spatiotemporal solitons are difficult to realize in practice because they must be launched with precise input conditions. Given the self-imaging property of a GRIN medium, we know that any CW beam evolves in a periodic fashion with a relatively small period of < 1mm. This suggests that we may be able to find solitons that maintain a constant temporal width, but whose spatial width follows a periodic pattern along the medium's length.

Even though the following analysis can be extended to other beam shapes, we focus on a pulsed Gaussian beam, launched into a GRIN fiber with a planar wavefront at $z = 0$. In the CW case, the solution is given in Eq (28). To apply this CW solution to a pulsed Gaussian beam,we assume that the band width of the pulse is narrow enough that the spatial profile $F(\mathbf{r})$ of the beam is not affected much by the nonlinear effects. With this approximation, the solution of Eq (42) is sought in the form [31]

$$A(x, y, z, t) = F(x, y, z)\, A_t(z, t), \tag{44}$$

where, $A_t(z, t)$ describing the temporal evolution of pulses does not depend on the spatial coordinates x and y because this dependence is contained in the spatial part $F(x, y, z)$.

To obtain an equation for $A_t(z, t)$, we follow a procedure well known in the case of single-mode fibers [14], while keeping in mind that $F(x, y, z)$ is not the spatial profile of any specific mode but changes with z. When we substitute Eq (44) in Eq (42), we obtain

$$F_s\left[\frac{dA_t}{dz}+\beta_1\frac{dA_t}{dt}+\frac{i\beta_2}{2}\frac{d^2A_t}{dt^2}-ik_0n_2|F_s|^2|A_t|^2A_t\right],$$

$$+A_t\left[\frac{dF_s}{dz}+\frac{1}{2i\beta_0}\left(\frac{\partial^2F_s}{\partial x^2}+\frac{\partial^2F_s}{\partial y^2}\right)\frac{i\beta_0\Delta}{a^2}(x^2+y^2)F_s\right]=0 \tag{45}$$

The expression in the second line vanishes because F_s is its solution. We multiply Eq (45) with F_s^* and integrate over the transverse coordinates x and y. The final result can be written as [31]

$$\frac{\partial A_t}{\partial z}+\beta_1\frac{\partial A_t}{\partial t}+\frac{i\beta_2}{2}\frac{\partial^2A_t}{dt^2}+=i\bar{\gamma}(z)|A_t|^2A_t, \tag{46}$$

where $|A_t|^2$ has units of power and the effective nonlinear parameter is defined as

$$\bar{\gamma}(z)=\frac{k_0n_2}{A_{eff}(z)},\qquad A_{eff}(z)=\frac{\left(\iint_{-\infty}^{\infty}|F_s(\mathbf{r})|^2\,dx\,dy\right)^2}{\iint_{-\infty}^{\infty}|F_s(\mathbf{r})|^4\,dx\,dy}. \tag{47}$$

This is a remarkable result. It shows that the pulse evolution inside a GRIN fiber can be studied by solving a single NLS equation, even though multiple spatial modes may be propagating inside the fiber. The oscillating spatial width of the Gaussian beam, resulting from self-imaging, gives rise to an effective nonlinear parameter $\bar{\gamma}(z)$ that is also periodic in z. This is not surprising because the intensity at a given distance z depends on the beam's width, becoming larger when the beam compresses and smaller as it expands. One can interpret this effect as a spatially varying effective mode area.

The spatial integrals in Eq (47) can be performed analytically using the form of $F(\mathbf{r})$ in Eq (29).The result is

$$A_{eff}(z)=A_{eff}(0)f(z),\qquad f(z)=\cos^2(2\pi z/L_p)+C_f^2\sin^2(2\pi z/L_p). \tag{48}$$

The functional form of the factor $f(z)$ becomes obvious from the observation that $A_{eff}(z)$ at any location scales with the spatial width as $w^2(z)$. We can use this relation to define $\bar{\gamma}(z)=\gamma/f(z)$, where $\gamma=k_0n_2/A_{eff}(0)$ is the initial value at $z=0$. As a final step, we drop the subscript t from A_t and use the reduced time $T=t-\beta_1z$ to write Eq (46) in the form

$$\frac{\partial A}{\partial z}+\frac{i\beta_2}{2}\frac{\partial^2A}{\partial T^2}=\frac{i\gamma}{f(z)}|A|^2A, \tag{47}$$

This equation reduces to the standard NLS equation when $C_f=1$.

Similar to the case of single-mode fibers, Eq (49) needs to be modified for pulses shorter than a few picoseconds [14]. The reason is related to the nature of the nonlinear response of a material to an electromagnetic field. In general, the molecular vibrations also produce a nonlinear response, in addition to the electrons. This response, known as the Raman response, is delayed in time, compared to the nearly instantaneous response of electrons, and this delay becomes relevant for short optical pulses. The Raman response is included by replacing the nonlinear index change $(\delta n)_{NL}=n_2|A|^2$ in Eq (42) with

$$(\delta_n)_{NL}=(1-f_R)\,n_2|A|^2+f_R\int_0^{\infty}h_R(t')|A(\mathbf{r},t-t')|^2\,dt', \tag{50}$$

where f_R represents the fractional contribution of the delayed response and $h_R(t)$ is the Raman response whosefunctional form is governed by vibrations of silica molecules. Its use in Eq (42) leads to thee following modified form of the effective NLS equation given in Eq (49):

$$\frac{\partial A}{\partial z}-i\sum_{n\neq2}^{M}\frac{i^n\beta_n}{n!}\frac{\partial^nA}{\partial T^n}=\frac{i\gamma}{f(z)}\left[(1-f_R)|A|^2A+f_R\int_0^{\infty}h_R(t')|A(z,T-T')|^2\,dT'\right], \tag{51}$$

where we included the higher order dispersion terms in the Taylor expansion of $\beta(\omega)$, because the spectral width of ultrashort pulses becomes large enough that their contribution may not be negligible. Often, it

is sufficient to include the β_3 term by choosing $M = 3$, but the β_4 and higher-order terms may be needed, depending on the situation.

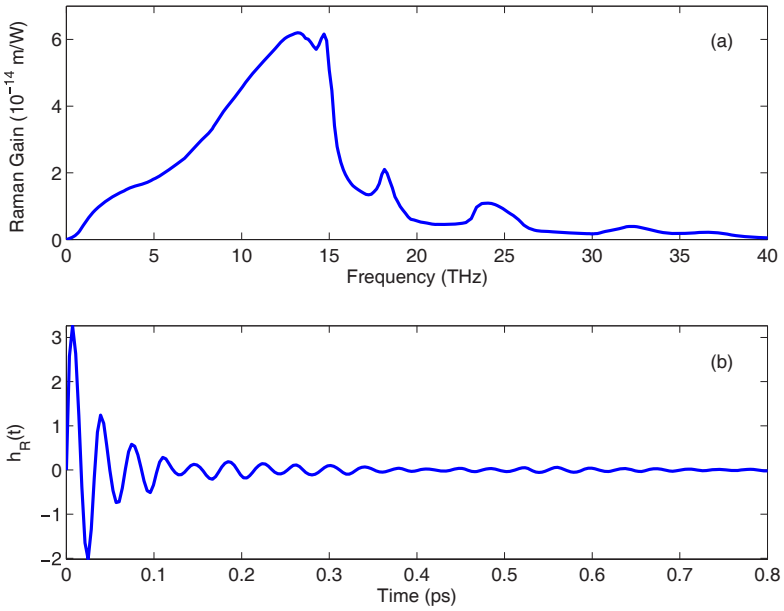

Fig 5. (a) Measured Raman gain spectrum of silica fibers; (b) temporal form of the Raman response function deduced from the gain data (from Ref.[14]).

The Raman response $h_R(t)$ in Eq (51) affects short pulses through the Raman gain. For pulses with a wide spectrum (>1THz), the Raman gain amplifies low-frequency components of a pulse by transferring energy from the high-frequency components of the same pulse.This phenomenon is called intrapulse Raman scattering. Because of it, the pulse spectrum shifts toward the low-frequency (red) side as the pulse propagates inside the fiber, a feature referred to as the Raman-induced self-frequency shift [14].

The functional form of the Raman response $h_R(t)$ depends on the Raman-gain spectrum that has been measured for silica fibers. Figure 5 shows (a) the experimental data and (b) the temporal form of $h_R(t)$ deduced from it [32]. Assuming a single vibrational frequency of silica molecules is involved in the Raman process, $h_R(t)$ can be approximated as [33]

$$h_R(t) = (\tau_1^{-2} + \tau_2^{-2})\,\tau_1 \exp(-t/\tau_2)\sin(t/\tau_1), \tag{52}$$

where τ_2 is the damping time of vibrations.The commonly used values for silica fibers are $\tau_1 = 12.2$ fs, $\tau_2 = 32$fs, and $f_R = 0.18$. A modified form of $h_R(t)$ was proposed in 2006 by Lin and Agrawal [34] to include the low-frequency hump seen in Fig 5.:

$$h_R^{new}(t) = (1 - f_b)\,h_R(t) + f_b\,[(2\tau_b - t)/\tau_b^2]\exp(-t/\tau_b), \tag{53}$$

where $f_b = 0.21$ and $\tau_b = 96$fs. This form requires $f_R = 0.245$ and explains better the observed Raman-induced frequency shifts of short optical pulses inside silica fibers.

7 Graded-Index Solitons

The question whether solitons can form inside multimode fibers attracted attention as early as 1980 [15,16]. It was realized that different group delays (or speeds) associated with different modes were likely to hinder the formation of such solitons. As intermodal group delays are relatively small for a GRIN fiber, it was

natural to consider soliton formation in such a medium. Indeed, theoretical work indicated that formation of temporal solitons was feasible inside a GRIN medium [17,18], By 2013, the formation of multimode solitons was observed in a GRIN fiber [10].

We use Eq (49) to find temporal solitons whose spatial shape evolves in a periodic fashion, as dictated by the phenomenon of self-imaging. It is clear from the presence of $f(z)$ in this NLS equation that perfect solitons cannot form inside GRIN fibers because Eq (49) is not integrable by the inverse scattering method. It was shown in 2018 that GRIN fibers support propagation of optical pulses that preserve their temporal shape and behave like a soliton, even though their spatial width oscillates along the fiber's length [20]. Such pulses are referred to as the GRIN solitons to emphasize that a parabolic index profile is essential for their existence.

Before, solving Eq (49) approximately, it is useful to normalize it using the variables

$$\tau = T/T_0, \qquad \xi = z/L_D, \qquad U = A/\sqrt{P_0}, \tag{54}$$

where, T_0 and P_0 are the width and the peak power of input pulses, respectively and $L_D = T^2/|\beta_2|$ is the dispersion length. The normalized NLS equation takes the form

$$i\frac{\partial U}{\partial \xi} + \frac{1}{2}\frac{\partial^2 U}{\partial \tau^2} + \frac{N^2}{f(\xi)}|U|^2 U = 0, \tag{55}$$

where we assumed $\beta_2 < 0$ and introduced the soliton order as $N = (\gamma P_0 L_D)^{1/2}$. The periodically varying function $f(z)$ given in Eq (48) can be written as,

$$f(\xi) = \cos^2(2\pi q\xi) + C_f^2 \sin^2(2\pi q\xi), q = L_D/L_p, \tag{56}$$

where, L_p is the self-imaging period. As $L_p \ll L_D$ in most cases, q is a large number ($q > 100$) under typical experimental conditions. Physically, it represents the number of times the spatial beam width oscillates inside a GRIN fiber within one dispersion length.

The dispersion length provides the scale over which solitons evolve. For this reason, solitons cannot respond to beam width changes taking place on a scale of 1mm or less when L_D exceeds 10cm. If we write the solution of Eq (55) as $U = \bar{U} + u$, where $\bar{U}$ represents average over one spatial period z_p, the perturbations $u(\xi, \tau)$ induced by spatial beam-width variations remain small enough that they can be neglected (as long as $q \gg 1$). In other words, the average dynamics of the soliton can be captured by solving the averaged NLS equation

$$i\frac{\partial \bar{U}}{\partial \xi} + \frac{1}{2}\frac{\partial^2 \bar{U}}{\partial \tau^2} + \bar{N}^2|\bar{U}|^2 \bar{U} = 0, \tag{57}$$

where, $\bar{N}$ is the effective soliton order defined as

$$\bar{N}^2 = N^2 \langle f^{-1}(\xi)\rangle = N^2/C_f. \tag{58}$$

It follows that Eq (57) has a solution in the form of a fundamental soliton when we choose $\bar{N} = 1$ or $N = \sqrt{C_f}$. This solution exists for a wide range of pulse widths as long as the peak power of pulses is adjusted to satisfy this soliton condition. As discussed before, C_f represents the fraction by which the beam width shrinks at $z = L_p/4$ before recovering its original width at $z = L_p/2$. Because of an oscillating beam width, the input peak P_0 must be adjusted to make sure that $\bar{N} = 1$ on average along the GRIN fiber.

Figure 6 compares the temporal and spectral profiles of a fundamental GRIN soliton ($\bar{N} = 1$), after it has propagated a distance of 100 L_D inside a GRIN fiber using $C_f = 0.2$ and $q = 100$. These results were obtained by solving Eq (55) numerically with the initial field $U(0,\tau) = U_0\,\mathrm{sech}(\tau)$, where U_0 was chosen to ensure $N = 1$. On the logarithmic scale, perturbations induced by spatial oscillations are evident, but their magnitude remains below the 50dB level even after100 dispersion lengths. Higher-order solitons for which

both the spatial and temporal widths evolve periodically can also form inside GRIN fibers. Numerical results indicate that higher-order solitons are less stable compared to the fundamental GRIN soliton [20]. They also undergo breakup into multiple fundamental solitons if third-order dispersion is included in Eq (55).

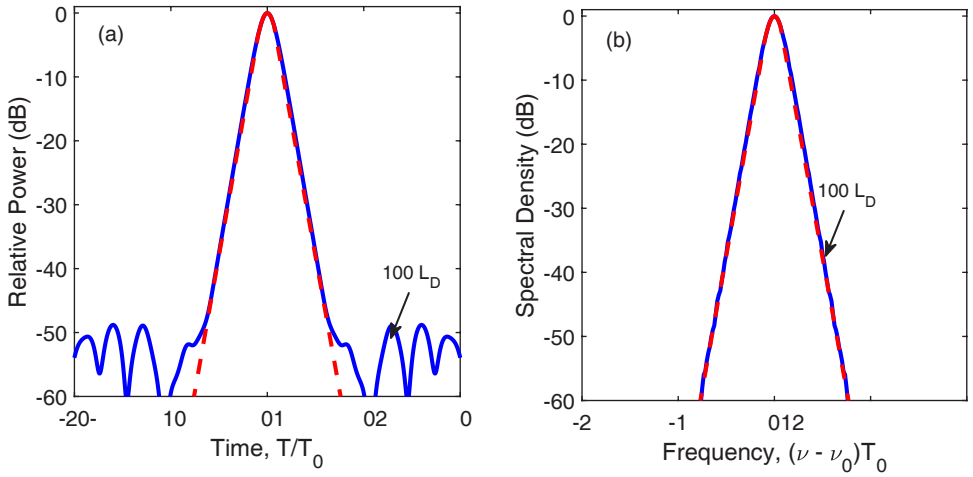

Fig 6. Temporal and spectral profiles of a multimode soliton ($\bar{N} = 1$) before (dashed line) and after it has propagated a distance of $100LD$ inside a GRIN fiber with $C_g^2 = 0.2$ and $q = 100$.

A GRIN soliton was observed in a 2013 experiment by launching 300 fs pulses (wavelength near 1550 nm) into a 100m-long GRIN fiber. [10]. At a specific pulse energy of 0.5 nJ, the input and output pulses had nearly the same temporal shapes, but the spectra were different because of different spectral shifts of different modes.The temporal width of this soliton reach a constant value of about 200 fs after some initial oscillations. Later numericaland experimental work included more modes and presented evidence of multimode solitons composed of five or more modes [35]. By 2021, a systematic study of GRIN solitons showed that the the predictions of Eq (57) do not always agree with the experiments [22-24]. The reason is understood by noting that Eq (57) ignores not only the spatiotemporal coupling but also intrapulse Raman scattering that plays a significant role for short optical pulses used in the experiments.

As discussed in Section 6, Eq (51) includes intrapulse Raman scattering. If we normalize this equation as indicated in Eq (54) and average over one self-imaging period, we can write it in the form

$$i\frac{\partial U}{\partial \xi} + \frac{1}{2}\frac{\partial^2 U}{\partial \tau^2} - i\delta_3 \frac{\partial^3 U}{\partial \tau^3} + \frac{N^2}{C_f}\left[(1-f_R)\,|U|^2 A + f_R U \int_0^\infty h_R(t')\,|U(z,\, T-T')|^2\, dT'\right] = 0, \tag{59}$$

where we used $M = 3$ and defined a third-order dispersion parameter as $\delta_3 = \beta_3/(6\beta_2 T_0)$. This equation allows us to consider the Raman-induced spectral shift of short pulses inside GRIN fibers. It can be solved numerically using the form of the Raman response given in Eq (53). It is found that the Raman-induced spectral shift is enhanced in GRIN fibers, compared to step-index fibers, because of the periodic spatial compression of a pulsed optical beam inside such fibers [36].

Figure 7 shows the impact of intrapulse Raman scattering on the (a) temporal and (b) spectral evolution of a soliton over a distance of $10L_D$ using $\delta_3 = 0.02$, $N = 1$, and $C_f = 0.5$. The soliton's spectrum in part (b) shifts toward lower frequencies in a continuous fashion because of the Raman-induced transfer of energy from high to low frequencies.The soliton's trajectory in part (a) bends toward the right side because of its continuous slowing down resulting from this spectral shift. Both of these features depend on the spatial compression factor C_f and are enhanced compared to the $C_f = 1$ case for which the spatial width remains constant.

The formation of GRIN solitons was investigated in a 2021 study by launching a pulsed Gaussian beam with the15-μm spot size into a 120m long GRIN fiber with 25μm core radius such that the energy of each pulse excited three LG_{0m} modes [24]. The width of pulses were in the 60–240 fs range and their wavelengths varied from 1300 -1700 nm. In most cases,the width of solitons was near 260fs when the energy of input pulses was in range of 2 to 6 nJ. Intrapulse Raman scattering played a substantial role in the formation of such solitons, and their wavelength at the fiber's output was considerably longer (by as much as 400nm) than the wavelength of input pulses. It was found that most of the energy of solitons was in the fund-amental mode at the output end of the GRIN fiber.

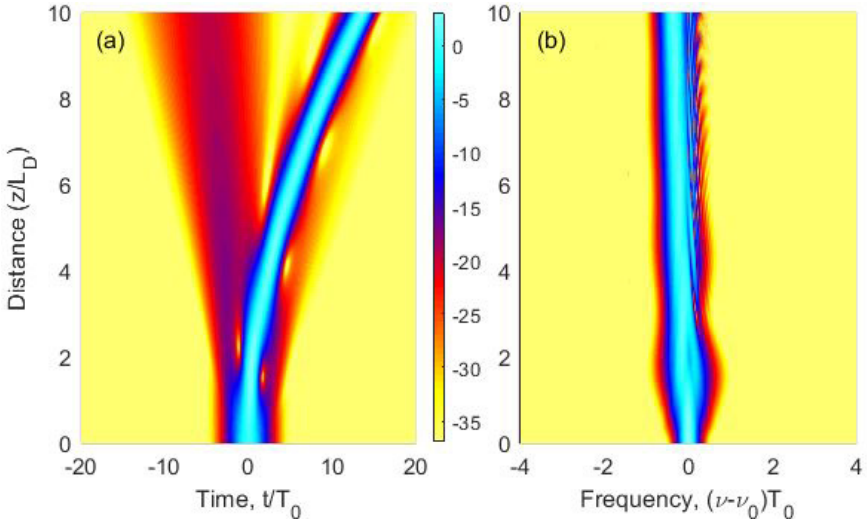

Fig 7. (a) Temporal and (b) spectral evolution of a soliton over a distance of 10*LD* for $\delta_3 = 0.02$, $N = 1$, and $C_f = 0.5$. Soliton's trajectory on the left bends because of the Raman-induced spectral shift seen in part (b).

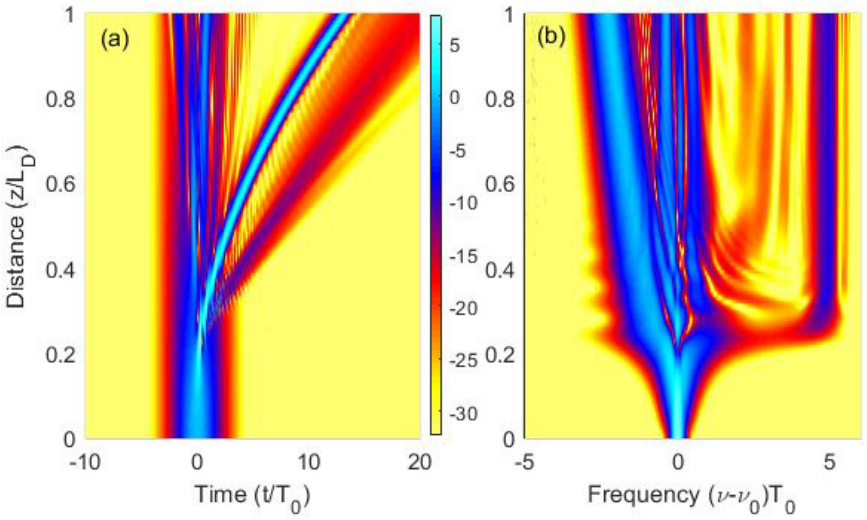

Fig 8. (a) Temporal and (b) spectral evolution of a third-order soliton ($N = 3$) over one dispersion length for $\delta_3 = 0.02$ and $C_f = 0.5$. Fission of this solitons broadens the spectrum and results in three fundamental solitons of different widths.

It is well known that higher-order solitons of the NLS equation, forming in single-mode fibers when the soliton order N exceeds 1, and they follow a periodic evolution pattern [14] with a period $(\pi/2)L_D$. In the presence of higher-order effects, such as TOD and intrapulse Raman scattering, these solitons undergo a fission process that breaks them into multiple fundamental ($N = 1$) solitons of different widths.We expect the fission of higher-order solitons to occur even in the case of GRIN fibers because the underlying dynamics remains the same, except for the enhancement of the nonlinear effects when the spatial width shrinks in each self-imaging period [22].

Figure 8 shows the (a) temporal and (b) spectral evolution of a third-order soliton (N =3) over the range $\xi = 0 - 1$ for $\delta_3 = 0.02$ and $C_f = 0.5$. The periodic evolution does not occur because of the fission of the third-order soliton near $\xi = 0.25$, that is initiated by intrapulse Raman scattering.This soliton breaks into three fundamental solitons of different widths.The spectrum of each new soliton shifts toward lower frequencies and it slows down; the shortest soliton has the largest spectral shift and slows down the most. A new feature is the appearance of a blue-shifted peak in the spectrum at the time of soliton fission.This peak belongs to a dispersive wave, generated when the soliton sheds radiation because of its perturbation by third-order dispersion.These features are well known in the context of single-mode fibers [14].

8 Concluding Remarks

In this article, written to honor the contributions of Prof Bishnu Pal to Optics and Photonics, I have discussed how he introduced me to the work on optical waveguides carried out during my Ph D days at IIT Delhi. A paper that I coauthored with Prof Ghatak in 1974 has turned out to be still relevant to those studying the nonlinear effects inside GRIN fibers. It was found in the 1974 paper that, even though an input beam incident on a GRIN fiber may excite hundreds of modes, the optical field at any point inside the fiber can be written, without any reference to the fiber modes, using a propagation kernel that is similar to that found in diffraction theory. This kernel shows that any input beam undergoes periodic compression and expansion such that its exact shape is reproduced along the length of a GRIN fiber (self-imaging) at distances separated by < 1 mm in typical GRIN fibers.The physical origin of self-imaging lies in a ladder-like structure of the modal propagation constants with equal spacing between any two neighboring modes of a GRIN medium with a parabolic index profile were used to derive the propagation kernel that governs evolution of CW beams inside a GRIN medium. I used this kernel to discuss first the self-imaging phenomenon and then to consider how a CW Gaussian beam evolves inside a GRIN fiber under the on-axis and off-axis launch conditions. Evolution of a pulsed Gaussian beam was discussed using a non-modal approach, resulting in a four-dimensional propagation equation, which could be extended to include the Kerr nonlinearity, responsible for both the self-focusing and self-phase modulation. The resulting equation was solved approximately to obtain an effective nonlinear Schrödinger equation that included the effects of periodic self-imaging. I used it to discuss the formation of fundamental and higher-ordersolitons inside a GRIN waveguide.The impact of intrapulse Raman scattering was also considered.

References

1. Agrawal G P, Ghatak A K, Mehta C L, Propagation of a partially coherent beam through Selfoc fibers, *Opt Comun*, 12 (1974)333–337.
2. Jacomme L, Modal dispersion in multimode graded-index fibers, *Appl Opt*, 14(1975)2578–2584.
3. Agrawal G P, Imaging characteristics of square law media, *Nouv Revued'Optique*, 7(1976)299–303.
4. Olshansky R, Propagation in glass optical waveguides, *Rev Mod Phys*, 51(1979)341–367.
5. Iga K, Theory for gradient-index imaging, *Appl Opt*, 19(1980)39–1043.
6. Richardson D J, Space-division multiplexing in optical fibres, *Nat Photon*, 7(2013)354–362.

7. Essiambre R.-J, Ryf R, Fontaine N K, Randel S, Space-division multiplexing in multimode and multicore fibers for high-capacity optical communication, *IEEE Photon J*, 5, 0701307(2013); doi.10.1109/JPHOT.2013.2253091.
8. Agrawal G P, Fiber-Optic Communication Systems, 5th edn, (Wiley), 2021.
9. Maf A, Pulse propagation in a short nonlinear graded-index multi-mode optical fiber, *J Light Technol*, 30 (2012)2803–2811.
10. Renninger W H, Wise F W, Optical solitons in graded-index multimode fibres, *Nature Commun*, 4,1719(2013); doi.org/10.1038/ncomms2739.
11. Krupa K, Tonello A, Barthélémy A, Couderc V, Shalaby B M, Bendahmane A, Millot G, Wabnitz S, Observation of geometric parametric instability induced by the periodic spatial self-imaging of multimode waves, *Phys Rev Lett*, 116(2016)183901; doi.org/10.1103/PhysRevLett.116.183901.
12. Wright L G, Ziegler Z M, Lushnikov P M, Zhu Z, Eftekhar P M, Christodoulides D N, Wise D N, Multimode nonlinear fiber optics: massively parallel numerical solver, tutorial, and outlook, *IEEEJ Sel Top Quantum Electron*, 24(2018)1–16.
13. Krupa K, Tonello A, Barthélémy A, Mansuryan T, Couderc V, Millot G, Grelu P, Modotto D,Wabin S A,Wabnitz S, Multimode nonlinear fiber optics, a spatiotemporal avenue, *APL Photonics*, 4,110901(2019); doi.org/10.1063/1.5119434.
14. Agrawal G P, Nonlinear Fiber Optics, 6th edn, (Academic Press), 2019.
15. Hasegawa A, Self-confinement of multimode optical pulse in a glass fiber, *Opt Lett*, 5(1980)416–417.
16. Crosignani B, Porto P D, Soliton propagation in multimode optical fibers, *Opt Lett*, 6(1981)329–330.
17. Yu S.-S, Chien C.-H, Lai Y, Wang J, Spatiotemporal solitary pulses in graded-index materials with Kerr nonlineary, *Opt Commun*, 119(1995)167–170.
18. Raghavan S, Agrawal G P, Spatiotemporal solitons in inhomogeneous nonlinear media, *Opt Commun*, 180(2000)377–382.
19. Kivshar Y S, Agrawal G P, Optical Solitons: From Fibers to Photonic Crystals, (Academic Press, 2003), Chap 7.
20. Ahsan A S, Agrawal G P, Graded-index solitons in multimode fibers, *Opt Lett*, 43(2018)3345–3348.
21. Agrawal G P, Self-imaging in multimode graded-index fibers and its impact on the nonlinear phenomena, *Opt Fiber Technol*, 50(2019)309–316.
22. Zitelli M, Mangini F, Ferraro M, Niang A, Kharenko D, Wabnitz S, *Opt Express*, 28(2020)20473–20488.
23. Zitelli M, Ferraro F, Mangini F, Wabnitz S, *Photon Res*, 9(2021)741–748.
24. Zitelli M, Ferraro M, Mangini F, Sidelnikov O, Wabnitz S, *Commun Phys*, 4(2021)182; doi.org/10.1038/s42005-021-00687-0.
25. Bliokh K Y, Rodriguez-Fortuño F J, Nori F, Zayats A V, Spin-orbit interactions of light, *Nat Photonics*, 9(2015) 796–808.
26. Chakravarthy T P, Viswanathan N K, Direct and reciprocal spin-orbit interaction effects in a graded-index medium, OSA Continuuum, 38(2021)2180–2186.
27. Ghatak A, Thyagarajan K, An Introduction to Fiber Optics, (Cambridge University Press),1999.
28. Olshansky R, Keck D B, Pulse broadening ingraded-index optical fibers, *Appl Opt*, 15(1976)483–491.
29. Thyagarajan K, Ghatak A K, Pulse broadening in optical fibers, *Appl Opt*, 16(1977)2583–2585.
30. Marcuse D, Theory of Dielectric Optical Waveguides, 2nd edn, (Academic Press), 1991.
31. Conforti M, Arabi C M, Mussot A, Kudlinski A, Fast and accurate modeling of nonlinear pulse propagation in graded-index multimode fibers, *Opt Lett*, 42(1017)4004–4007.
32. Stolen R H, Gordon J P, Tomlinson W J, Haus H A, Raman response function of silica-core fibers, *J Opt Soc Am B*, 6(1989)1159–1166.
33. Blow K J, Wood D, Theoretical description of transient stimulated Raman scattering in optical fibers, *IEEE J Quantum Electron*, 25(1989)2665–2673.
34. Linand Q, Agrawal G P, Raman response function for silica fibers, *Opt Lett*, 31(2006)3086–3088.

35. Wright L G, Wabnitz S, Christodoulides D N, Wise F W, Ultrabroadband dispersive radiation by spatiotemporal oscillation of multimode waves, *Phys Rev Lett*, 115(2015)223902; doi.org/10.1103/PhysRevLett.115.223902.

36. Ahsan A S, Agrawal G P, Spatio-temporal enhancement of Raman-induced frequency shifts in graded-index multi-mode fibers, *Opt Lett*, 44(2019)2637–2640.

[*Received*: 13.12.2021; *accepted*: 01.01.2022]

Govind P Agrawal received the B.Sc. degree from the University of Lucknow in 1969 and the M.Sc.and Ph D degrees from the Indian Institute of Technology, New Delhi in 1971 and 1974, respectively. After holding positions at EcolePolytechnic, France, City University of NewYork, and Bell Laboratories, N J, Dr Agrawal joined in 1989 the faculty of the Institute of Optics at the University of Rochester,where he holds the positions of Professor of Optics, Professor of Physics, and LLE Senior Scientist.His research interests span from optical communications and semiconductor lasers to nonlinear fiberoptics and silicon photonics. He is an author or coauthor of more than 450 research papers and nine books including Fiber-Optic Communication Systems (4th edn.,Wiley 2010) and Nonlinear Fiber Optics (6th edn, Academic Press 2019).These two books are used worldwide for graduate teaching and have helped in training a whole generation of scientists. Dr Agrawal is a Fellow of the Optical Society of America (OSA) and a Life Fellow of the Institute of Electrical and Electronics Engineers (IEEE). He is also a Fellow of the Optical Society of India. From 2008 to 2010 Dr Agrawal chaired the Publication Council of OSA and was a member of its Board of Directors. From 2014 to 2019 he served as the Editor-in-Chief of the OSA Journal Advances in Optics and Photonics. His almamater, Indian Institute of Technology, gave him in 2000 its Distinguished Alumni Award. In 2012, IEEE Photonics Society honored him with its Quantum Electronics Award. He received the 2013 William H Riker University Award for Excellence in Graduate Teaching. In 2015, he was awarded the Esther Hoffman Beller Medal of the Optical Society. Dr Agrawal was the recipient of two major awards in 2019: Max Born Award of the Optical Society and Quantum Electronics Prize of the European Physics Society.